

# Investigation Of Nanoscale Dielectric Polarization And Refractive Indices Of BaTiO<sub>3</sub> Surfaces And Ultrathin Films

H. Chaib<sup>1,\*</sup>, L. M. Eng<sup>2</sup>, A. Nafidi<sup>3</sup>, A. Khalal<sup>3</sup>, A. Tirbiyine<sup>4</sup>, and A. Taoufik<sup>4</sup>

<sup>1</sup> Polydisciplinary Faculty, Ibn Zohr University, P.O. Box 83, 45002 Ouarzazate, Morocco;

<sup>2</sup> Institute of Applied Photophysics, University of Technology, D-01062 Dresden, Germany;

<sup>3</sup> Condensed Matter Physics Group, Faculty of Sciences, Ibn Zohr University, Agadir, Morocco;

<sup>4</sup> Group of High Critical Temperature Superconductor Materials, Faculty of Sciences, Ibn Zohr University, Agadir, Morocco

\* Corresponding author: hchaib@gmail.com

**Abstract** : The surface and interface effects on the dielectric polarization and refractive indices of BaTiO<sub>3</sub> single crystals and BaTiO<sub>3</sub> ultrathin films on SrTiO<sub>3</sub> single crystal substrates are investigated theoretically by using a microscopic model based on the orbital approximation in correlation with the dipole-dipole interaction. The spontaneous polarization of BaTiO<sub>3</sub> single crystals is drastically reduced near the c-surface. For BaTiO<sub>3</sub>/SrTiO<sub>3</sub> films, the spontaneous polarization is reduced in the film as its thickness decreases. However, an electronic polarization appears within the SrTiO<sub>3</sub> substrate in the neighborhood of the interface. This polarization, which vanishes far away from the interface into the SrTiO<sub>3</sub> bulk, is induced by the polarization of the BaTiO<sub>3</sub> film. Furthermore, we find the refractive index either for BaTiO<sub>3</sub> single crystals or for BaTiO<sub>3</sub> films and SrTiO<sub>3</sub> substrates to be strongly reduced for light polarized perpendicular to the surface.

## I. Introduction

Tetragonal barium titanate (BaTiO<sub>3</sub>) is a ferroelectric oxide material of great importance for potential applications due to its unusual piezoelectric, ferroelectric, dielectric, optical, electro-optic, and photorefractive properties. Many of these applications are increasingly oriented towards thin films [1-11] and superlattice geometries [12-21], where surface/interface properties are of growing importance. Strontium titanate (SrTiO<sub>3</sub>) is one of the materials of choice for growing BaTiO<sub>3</sub> thin films as well as for stacking BaTiO<sub>3</sub>/SrTiO<sub>3</sub> superlattices due to the relatively low atomic misfit between the two. At room temperature, SrTiO<sub>3</sub> is a centrosymmetric paraelectric material with a cubic structure having a lattice parameter ( $a=3.905\text{\AA}$ ) [5] close to that of tetragonal BaTiO<sub>3</sub> ( $a=3.992\text{\AA}$  [22]) with a difference of about 2%. This mismatch between the in-plane lattice parameters of BaTiO<sub>3</sub> and SrTiO<sub>3</sub> is the reason of the lattice strain induced in the thin BaTiO<sub>3</sub> films as well as in periodically stacked layers within the superlattice structures.

Here we use a quantum mechanical theoretical approach for studying the room temperature spontaneous polarization and refractive indices of BaTiO<sub>3</sub> single crystals at the c-oriented surface and those of BaTiO<sub>3</sub> thin films grown on SrTiO<sub>3</sub> substrates. Our microscopic model takes into account the anisotropy in the first-, second-, and third-order

electronic polarizabilities of all constituent ions, their ionic shifts as well as the crystalline deformations. The model was previously tested for the calculation of bulk properties of mono-domain tetragonal perovskites like tetragonal BaTiO<sub>3</sub> and KNbO<sub>3</sub>, i.e. their ferroelectricity and optical anisotropy as well as their linear electro-optic coefficients [23]. Furthermore the same model was successfully applied for modeling electrical and optical properties of rhombohedral LiNbO<sub>3</sub> single crystals, as well as 90° and 180° ferroelectric domain walls and surface effects in BaTiO<sub>3</sub> [24]. Based on those experiences which agree very well with the corresponding experimental data, we initiate here the application of this model to BaTiO<sub>3</sub> single crystal surfaces and thin films in tetragonal phase.

The paper is structured as follows: Section 2 contains a brief summary of the technical details of the work, including the used theoretical method. In section 3, we present the results of the spontaneous polarization and refractive indices computed at room temperature for BaTiO<sub>3</sub> surfaces and BaTiO<sub>3</sub>/SrTiO<sub>3</sub> ultrathin films. This section also contains the discussion of the above-mentioned findings.

## II. Theoretical preliminaries

In our computation we have to solve the following sets of equations (see [24] for more details):

$$\sum_{j=1}^5 \sum_{l=1}^3 \sum_{\tilde{m}} S_{kl}(\tilde{n}, \tilde{m}) E_l^{\text{loc}}(\tilde{m}) = Q_k(\tilde{n}) \quad (1)$$

and

$$\sum_{j=1}^5 \sum_{l=1}^3 \sum_{\tilde{m}} S_{kl}^*(\tilde{n}, \tilde{m}) \frac{\partial E_l^{\text{loc}}(\tilde{m})}{\partial E_{l'}^{\text{opt}}} = \delta_{kl'} \quad (2)$$

where  $Q_k(\tilde{n})$  represents the contribution of the external electric field and the ionic dipole moment of all ions in the sample to the  $l$ -component of the local electric field of the  $i$ -ion located in the  $\tilde{n}$ -unit cell. The factors  $S_{kl}(\tilde{n}, \tilde{m})$  and  $S_{kl}^*(\tilde{n}, \tilde{m})$  are defined in such a way that  $S_{kl}(\tilde{n}, \tilde{m}) E_l^{\text{loc}}(\tilde{m})$  represents the opposite of the contribution of the  $l$ -component of the electronic dipole moment of the  $j$ -ion located in the  $\tilde{m}$ -unit cell to the  $k$ -component of the local electric field of the  $i$ -ion located in the  $\tilde{n}$ -unit cell and  $S_{kl}^*(\tilde{n}, \tilde{m}) \cdot \partial E_l^{\text{loc}}(\tilde{m}) / \partial E_{l'}^{\text{opt}}$  represents the opposite of the contribution of the  $l$ -component of the induced electronic dipole moment of the  $j$ -ion located in the  $\tilde{m}$ -unit cell by unit of optical electric field to the  $k$ -component of the induced local electric field of the  $i$ -ion located in the  $\tilde{n}$ -unit cell by unit of optical electric field. Please, note that the elements of the tensors  $\tilde{Q}$ ,  $\tilde{S}$ , and  $\tilde{S}^*$  can be computed by using the static effective charges of the constituent ions, their first-, second-, and third-order electronic polarizabilities, as well as the crystallographic properties (i.e. lattice parameters and ionic shifts) of the sample. However, it is noteworthy that there is a mutual dependence between the first-, second-, and third-order electronic polarizabilities (orbital approximation) on one hand, and their dependence on the electric field (dipole-dipole interaction) on the other hand, which makes a self-consistent calculation necessary.

In fact, by solving the sets of equations given by Eq. (1) we obtain the local electric field,  $E_l^{\text{loc}}$ , and its derivative with respect to the optical electric field,  $\partial E_l^{\text{loc}} / \partial E_{l'}^{\text{opt}}$ , for all ions in each unit cell. Therefore, the spontaneous polarization and refractive indices for every unit cell in the sample is readily deduced using these two computed magnitudes (i.e.  $E_l^{\text{loc}}$  and  $\partial E_l^{\text{loc}} / \partial E_{l'}^{\text{opt}}$ ).

By considering only the 86 unit cell monolayers nearest to the sample surface and taking into account that all unit cells in the same monolayer have the same properties, the number of equations in each set of equations can be reduced to  $3 \times 5 \times 86 = 1290$  equations. The wavelength at which our optical properties (i.e.

the refractive indices and optical birefringence) have been computed is  $\lambda = 589.3$  nm, purposely chosen to coincide with the availability of literature data for the free electronic polarizabilities. Treating the full spectral response of the BaTiO<sub>3</sub> and SrTiO<sub>3</sub> systems would need the Schrödinger equation to be solved time dependently, which is beyond the scope of this paper.

### III. Results and discussion

#### III-1. BaTiO<sub>3</sub> surfaces

The calculation of the spontaneous polarization and refractive indices is carried out for c-domain areas in tetragonal BaTiO<sub>3</sub> at room temperature by using the lattice parameters and spontaneous ionic shifts given in [25]. As static effective charges, we use the data published in a recent theoretical work devoted to the quantitative study of successive phase transitions in BaTiO<sub>3</sub> [26], [27]:  $Z_{33}^{\text{ss}}(\text{Ba}^{2+}) = 1.437$ ,  $Z_{33}^{\text{ss}}(\text{Ti}^{4+}) = 2.063$ ,  $Z_{33}^{\text{ss}}(\text{O}_{x,y}^{2-}) = -1.200$ , and  $Z_{33}^{\text{ss}}(\text{O}_z^{2-}) = -1.100$ . It is noteworthy that, for symmetry reasons, the static effective charge tensors of the constituent ions of tetragonal BaTiO<sub>3</sub> have to be diagonal, and consequently the non-diagonal elements  $Z_{kl}^{\text{ss}}$  are zero. Moreover, the components  $Z_{11}^{\text{ss}}$  and  $Z_{22}^{\text{ss}}$  of the static effective charge tensors have no effect in the calculation because the static effective charges are coupled with the ionic shifts which are parallel to the 3-direction. It is assumed that these magnitudes (lattice parameters, static effective charges and ionic shifts) are valid both near the surface and in the bulk.

Firstly, we present and discuss the results obtained for the spontaneous polarization which is ascribed to the unit cell (and not to individual ions) and is defined as the total dipole moment (in the unit cell) per volume. The calculation shows that the values of the spontaneous polarization near the c-surface of tetragonal BaTiO<sub>3</sub> at room temperature along the 1- and 2-directions are exactly zero. On the other hand, the 3-component of the spontaneous polarization is nonzero and is reported in Fig. 1-(a) for the c-surface (TiO<sub>2</sub>-terminated).

The values of the spontaneous polarization near and far away from the c-surface (inside the bulk) do not change when varying the radius  $R^{\text{cav}}$  of the spherical Lorentz cavity but they change in between. In fact, the larger  $R^{\text{cav}}$  the more accurate is the calculation since more interacting unit cells are considered. However, increasing  $R^{\text{cav}}$  further in our calculation is currently impossible due to extremely long computation time.

Fig. 1-(b) reports the calculated values for the refractive indices ascribed to each unit cell near the  $c^-$ -surface ( $\text{TiO}_2$ -terminated) of tetragonal  $\text{BaTiO}_3$  at room temperature. Note that the calculated results are displayed as the discrete values for the refractive indices making sense on the unit cell bases only (and not on the ionic scale). When approaching the  $c^-$ -surface ( $\text{TiO}_2$ -terminated), the refractive index  $n_3$ , corresponding to light polarized perpendicular to the sample surface, undergoes a very strong decrease. It decreases from 2.32 inside the bulk (far away from the surface) to  $\sim 1.73$  close to the surface. Note that near the  $c^-$ -surface the refractive indices  $n_1$  and  $n_2$  coincide with each other (i.e.,  $n_1 = n_2$ ).

The unit cell monolayer closest to the surface for the studied  $c^-$ -surface presents an exception with respect to the other unit cell monolayers for the refractive indices corresponding to light being polarized parallel to the surface (i.e.  $n_1$  and  $n_2$ ). This exception manifests in the discontinuous decrease of the concerned refractive indices of the unit cell monolayer closest to the sample surface.

Far away from the surface and for whatever the value chosen for  $R^{\text{cav}}$ , the crystal possesses only two refractive indices, the ordinary refractive index  $n_o$  (which coincides with  $n_1 = n_2$ ), and the extraordinary refractive index  $n_e$  (which is  $n_3$ ). The calculated values of these indices are  $n_o = 2.385$  and  $n_e = 2.315$ , respectively, which are in good agreement with experimental data ( $n_o = 2.398$  and  $n_e = 2.312$ ) given by Johnston and Weingart [29] for single-domain tetragonal  $\text{BaTiO}_3$  at room temperature. Nevertheless, the material behaves near the  $c^-$ -surface like a uniaxial negative material with high optical birefringence,  $\Delta n = 0.55$ .

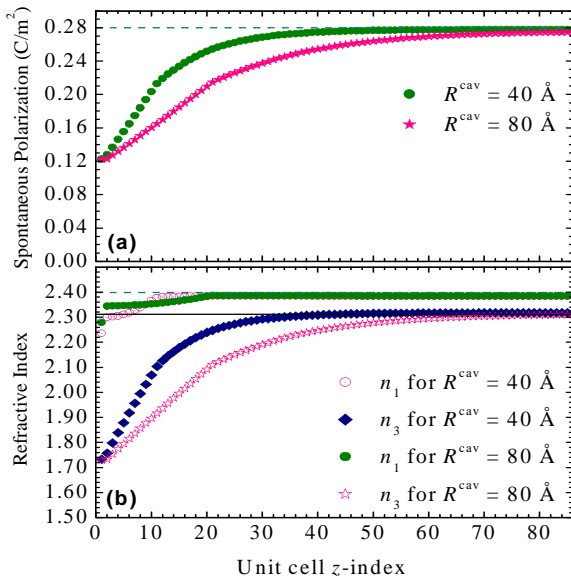


Fig. 1: Variation of the spontaneous polarization (a) and refractive indices (b) near the  $c^-$ -surface ( $\text{TiO}_2$ -terminated) of tetragonal  $\text{BaTiO}_3$ . Results are computed at room temperature with  $R^{\text{cav}} = 40 \text{ \AA}$  and  $R^{\text{cav}} = 80 \text{ \AA}$ . The dashed line in graph (a) represents the measured bulk single crystal spontaneous polarization according to Cudney [28]. The dashed and solid lines in graph (b) represent the measured single crystal values, respectively, of the ordinary and extraordinary refractive indices according to Johnston and Weingart [29].

Furthermore, the above reported calculations have been repeated, considering this time the other configurations of the surface (i.e. either  $c^+$  or  $c^-$  and either  $\text{BaO}$ - or  $\text{TiO}_2$ -terminated), instead of the  $\text{TiO}_2$ -terminated  $c^-$ -surface considered above. It is found that the behavior of the spontaneous polarization, for which the decrease near the  $c^-$ -surface reaches 57%, is the same for the four distinguished surface configurations. The only difference manifests in the effective value of the spontaneous polarization of the unit cell monolayer closest to the surface, which is slightly smaller for  $\text{BaO}$ -terminated (both  $c^-$  and  $c^+$ )-surfaces than for  $\text{TiO}_2$ -terminated (both  $c^-$  and  $c^+$ )-surfaces. Yet, the refractive indices  $n_1$  and  $n_2$  ( $n_1 = n_2$ ), for which the change near the  $\text{TiO}_2$ -terminated  $c^+$ -surface is apparent and is more pronounced for  $R^{\text{cav}} = 40 \text{ \AA}$  than for  $R^{\text{cav}} = 80 \text{ \AA}$ , remain almost constant when approaching the  $\text{BaO}$ -terminated  $c^\pm$ -surface.

### III-2. $\text{BaTiO}_3$ ultrathin films on $\text{SrTiO}_3$ substrate

The calculation of the spontaneous polarization and refractive indices is carried out for two different thicknesses (i.e. 10 and 20 ML; ML = monolayer) of a  $c$ -oriented  $\text{BaTiO}_3$  thin film on the  $\text{SrTiO}_3$  substrate at room temperature. In this calculation we take into account that the lattice parameter of the cubic substrate is  $a = 3.905 \text{ \AA}$ , the spontaneous ionic shifts are zero, and the static effective charges are [30]:  $Z_{kk}^{\text{ss}}(\text{Sr}^{2+}) = 1.852$ ,  $Z_{kk}^{\text{ss}}(\text{Ti}^{4+}) = 2.272$ , and  $Z_{kk}^{\text{ss}}(\text{O}_{x,y,z}^{2-}) = -1.375$  (note that the charge neutrality sum rule is fulfilled to 0.1%:  $\sum_{j=1}^5 Z_{jj}^{\text{ss}}(j) = -0.001$ ). The  $\text{BaTiO}_3$  thin film undergoes a lattice strain by keeping its tetragonal structure [4,7]. The lattice parameters of the thin film are  $a = b = 3.905 \text{ \AA}$  (coinciding with that of the  $\text{SrTiO}_3$  substrate) and  $c = v^{\text{blk}}/ab$  ( $v^{\text{blk}}$  is the volume of the bulk unit cell in  $\text{BaTiO}_3$  [4,7]), and the spontaneous ionic shifts are those given in [25]. As static effective charges of the film, we use the same data used in the previous subsection. It is noteworthy that for symmetry reasons the static effective charge tensors of the constituent

ions of both cubic SrTiO<sub>3</sub> and tetragonal BaTiO<sub>3</sub> have to be diagonal and consequently the non-diagonal elements  $Z_{kl}^{*s}$  are zero. The in-plane lattice parameters considered here for the thin film of 20 ML thickness are slightly different from those published by Yoneda *et al.* [4,7]. In fact, in order to simplify modeling, it is very important to assume that the in-plane lattice parameters of the BaTiO<sub>3</sub> film coincide exactly with those of the SrTiO<sub>3</sub> substrate, because the mismatch between the in-plane lattice parameters of the film and the substrate generates dislocations in the crystallographic structure of the film and then renders the modeling very complicated. However, the unit cell volume is independent of the film thickness for BaTiO<sub>3</sub> ultrathin films at room temperature as shown experimentally by Yoneda *et al.* [4,7]. It is also assumed that these magnitudes (lattice parameters, static effective charges, and ionic shifts) are valid both near the surface/interface and in the bulk.

Now we present and discuss the results obtained for the spontaneous polarization ascribed to each unit cell (and not to individual ions). The calculation shows that the values of the spontaneous polarization within the SrTiO<sub>3</sub> substrate and the BaTiO<sub>3</sub> ultrathin film at room temperature along the 1- and 2-directions are exactly zero. On the other hand, the 3-component of the spontaneous polarization is non-zero and is displayed in Fig. 2-(a) for the two film thicknesses of 10 and 20 ML (calculated for TiO<sub>2</sub>-terminated c<sup>-</sup>-surface).

The spontaneous polarization of the film increases when its thickness increases, achieving values of  $\sim 0.060$  and  $\sim 0.085 \text{ C/m}^2$  (mean values) for a 10 and 20 ML BaTiO<sub>3</sub> thin film on SrTiO<sub>3</sub> substrate. Moreover, the value of the spontaneous polarization within the film always decreases when approaching the surface. This decrease is mainly attributed to the surface effect, because the closer the ion gets to the BaTiO<sub>3</sub> surface, the more incomplete the Lorentz spherical cavity is, resulting in a smaller number of ions interacting with the ion considered. It has been shown in a recent experimental work [4] that the magnitude of the spontaneous polarization of BaTiO<sub>3</sub> film of 30 ML thickness is around  $0.03 \text{ C/m}^2$  which is smaller than that estimated from our calculation. This difference might be attributed to the depolarizing electric field induced within the film by the surface and interface charges [31,32].

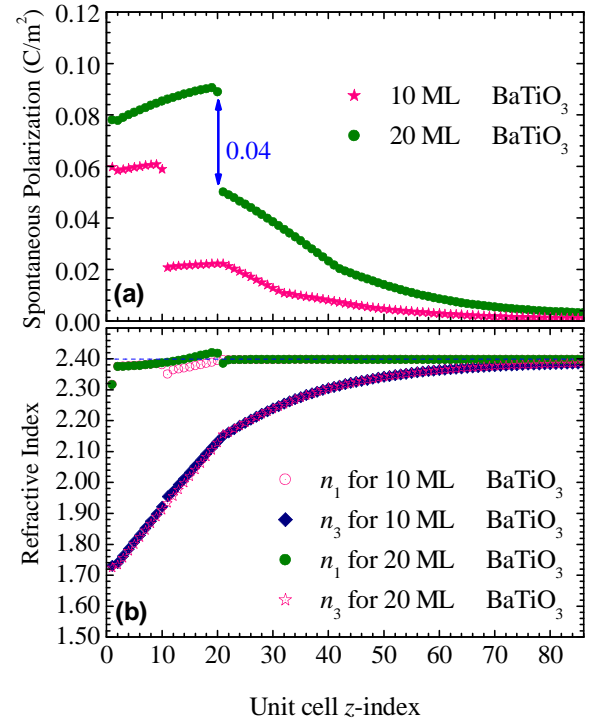


Fig. 2: Variation of the spontaneous polarization (a) and refractive indices (b) within the BaTiO<sub>3</sub> ultrathin film (TiO<sub>2</sub>-terminated c<sup>-</sup>-surface) and the SrTiO<sub>3</sub> substrate. Results are computed at room temperature for two different values of the film thickness, 10 and 20 ML. The Lorentz spherical cavity radius measures  $R^{\text{cav}}=80\text{\AA}$ . The dashed line represents the measured value of the refractive index of SrTiO<sub>3</sub> single crystals at 589.3 nm and room temperature according to Levin *et al.* as stated by Lawless in [33].

It appears that not only the BaTiO<sub>3</sub> film but also the SrTiO<sub>3</sub> substrate has a dielectric spontaneous polarization. This polarization is important near the BaTiO<sub>3</sub>/SrTiO<sub>3</sub> interface and decreases to zero far into the SrTiO<sub>3</sub> bulk. It is purely electronic because the ionic polarization is zero within the SrTiO<sub>3</sub> substrate (the substrate ionic polarization is zero because the ionic shifts are zero). We notice that the spontaneous polarization generated within the substrate is induced, through the dipolar interactions, by the dipole moments (polarized ions) existing within the film. It remains to note that the gap in the spontaneous polarization seen at the interface is due to the vanishing of the ionic polarization when passing from the BaTiO<sub>3</sub> film to the substrate. As seen in Fig. 2-(a), this polarization difference is almost independent of the film thickness and has a value of  $\sim 0.04 \text{ C/m}^2$ .

Fig. 2-(b) reports the calculated values for the refractive indices ascribed to each unit cell within the SrTiO<sub>3</sub> substrate and the BaTiO<sub>3</sub> ultrathin films (calculated for TiO<sub>2</sub>-terminated c<sup>-</sup>-surface) at room

temperature for the two different thicknesses considered. Note that the calculated results are displayed as discrete values for the refractive indices, making sense on the unit cell bases only (and not for individual ions). For both thicknesses of the ultrathin film, the  $n_3$  refractive index, which corresponds to light polarized perpendicular to the surface/interface, undergoes a very strong decrease when approaching the surface, without showing any discontinuity at the interface as is the case for the spontaneous polarization. Values range from 2.4 (which is the refractive index of the bulk of  $\text{SrTiO}_3$ ) inside the substrate (far away from the surface) to  $\sim 1.75$  close to the surface. However, the change undergone by the refractive indices  $n_1$  and  $n_2$  (which coincide with each other; i.e.  $n_1=n_2$ ), corresponding to light polarized in the plane parallel to the surface/interface, is very small. This change is manifested in a variation in both refractive indices near the surface accompanied by a small discontinuity at the interface. Furthermore, the refractive indices corresponding to light polarized parallel to the surface (i.e.  $n_1$  and  $n_2$ ) of the unit cell monolayer closest to the sample surface are slightly smaller than those of the other unit cell monolayers.

Far away from the surface into the  $\text{SrTiO}_3$  bulk, whatever the thickness of the film, the medium becomes isotropic as it possesses only one refractive index which coincides with that of the bulk of cubic  $\text{SrTiO}_3$  single crystals ( $n_0=2.4$  [33]). Nevertheless, the sample behaves near the surface like a uniaxial negative material with a high optical birefringence of  $\Delta n \sim 0.6$ .

Furthermore, the calculations relative to the ultrathin films reported above have been repeated, considering this time the other configurations of the film surface (i.e. either  $c^+$  or  $c^-$  and either  $\text{BaO}$ - or  $\text{TiO}_2$ -terminated), instead of the  $\text{TiO}_2$ -terminated  $c^-$ -surface considered above. It is found that for every thickness of the film, the behavior of the spontaneous polarization near the  $c$ -surface/interface are the same for the four configurations distinguished here ( $c^\pm$ -surfaces, both  $\text{BaO}$ - and  $\text{TiO}_2$ -terminated). However, two differences distinguish the film with the  $\text{BaO}$ -terminated surface from that with  $\text{TiO}_2$ -termination. The first one is manifested in the effective value of the spontaneous polarization of the  $\text{BaTiO}_3$  unit cell monolayer closest to the surface, which is smaller for  $\text{BaO}$ -terminated surfaces (both  $c^-$ - and  $c^+$ -surfaces) than for  $\text{TiO}_2$ -terminated surfaces (both  $c^-$ - and  $c^+$ -surfaces). The second aspect concerns the effective value of the spontaneous polarization of the  $\text{SrTiO}_3$  unit cell monolayer closest to the interface which is slightly larger for  $\text{BaO}$ -terminated surfaces (both  $c^-$ -

and  $c^+$ -surfaces) than for  $\text{TiO}_2$ -terminated surfaces (both  $c^-$ - and  $c^+$ -surfaces).

Our theoretical calculations show that the spontaneous polarization increases with the thickness of the thin film while the behavior of the refractive indices is almost the same whatever the thickness of the film. The spontaneous polarization is always parallel to the  $c$ -axis and its value decreases strongly when crossing the interface from the film towards the substrate. On the other hand, the refractive index corresponding to light polarized perpendicular to the sample surface undergoes an important change near the surface.

## IV. Conclusions

By using a microscopic model taking into account a quantum mechanical variation method based upon the orbital approximation and the dipole-dipole interaction due to the local electric field acting on the constituent ions, we calculated the electric and optical properties of  $\text{BaTiO}_3$  single crystals at the  $c$ -oriented surface of  $c$ -domain and of  $\text{BaTiO}_3$  thin films grown on  $\text{SrTiO}_3$  substrates at room temperature. The calculations show that the spontaneous polarization of the film increases with its thickness, as does that of the substrate in the neighborhood of the interface (i.e. the spontaneous polarization of the substrate unit cells close to the interface increases with increasing  $\text{BaTiO}_3$  film thickness), while the refractive index behavior remains almost the same on changing the thickness of the film. However, the magnitude of the spontaneous polarization of a ultrathin film of  $\text{BaTiO}_3/\text{SrTiO}_3$  is smaller than that for tetragonal  $\text{BaTiO}_3$  single crystals, indicating that the lattice strain and the surface/interface effects present induced polarization suppression as observed by Yoneda *et al.* in a recent experimental work [4].

Moreover, the spontaneous polarization of  $\text{BaTiO}_3$  single crystal as well as that of  $\text{BaTiO}_3$  ultrathin film decreases when approaching the surface and behaves quite similarly to what was found in a recent theoretical work based on Landau [31,34] and Landau-Ginzburg-Devonshire thermodynamic theory [35] and also from shell model calculations for ultrathin films [36]. Furthermore, the  $\text{BaTiO}_3$  single crystal and  $\text{BaTiO}_3/\text{SrTiO}_3$  ultrathin film behave, respectively, like a biaxial and uniaxial crystal, resulting in dramatic changes of the refractive index  $n_3$  near the surface/interface. This effect might be the main origin of the reduction of the refractive indices of  $\text{BaTiO}_3$  films observed in recent experimental work [8,11].

## V. References

- [1] Y. Watanabe, Y. Matsumoto, H. Kunitomo, M. Tanamura, and E. Nishimoto, *Jpn. J. Appl. Phys.* **33**, 5182 (1994).
- [2] H. Funakubo, D. Nagano, A. Saiki, Y. Inagaki, K. Shinozaki, and N. Mizutani, *Jpn. J. Appl. Phys.* **34**, 5879 (1997).
- [3] L. Xuan, S. Pan, Z. Chen, R. Wang, W. Shi, and C. Li, *Appl. Phys. Lett.* **73**, 2896 (1998).
- [4] Y. Yoneda, T. Okabe, K. Sakaue, and H. Terauchi, *J. Appl. Phys.* **83**, 2458 (1998).
- [5] T. Zhao, F. Chen, H. Lu, G. Yang, and Z. Chen, *J. Appl. Phys.* **87**, 7442 (2000).
- [6] T. Zhao, H. Lu, F. Chen, G. Yang, and Z. Chen, *J. Appl. Phys.* **87**, 7448 (2000).
- [7] Y. Yoneda, K. Sakaue, and H. Terauchi, *J. Phys.: Condens. Matter* **13**, 9575 (2001).
- [8] A. Petraru, J. Schubert, M. Schmid, and Ch. Buchal, *Appl. Phys. Lett.* **81**, 1375 (2002).
- [9] J. Junquera and P. Ghosez, *Nature* **422**, 506 (2003).
- [10] M. El Marssi, F. Le Marrec, I. A. Lukyanchuk, and M. G. Karkut, *J. Appl. Phys.* **94**, 3307 (2003).
- [11] J. Schubert, O. Trithaveesak, A. Petraru, C. L. Jia, R. Uecker, P. Reiche, and D. G. Schlom, *Appl. Phys. Lett.* **82**, 3460 (2003).
- [12] H. Tabata, H. Tanaka, T. Kawai, and M. Okuyama, *Jpn. J. Appl. Phys.* **34**, 544 (1995).
- [13] T. Zhao, Z. Chen, F. Chen, W. Shi, H. Lu, and G. Yang, *Phys. Rev. B* **60**, 1697 (1999).
- [14] T. Shimuta, O. Nakagawara, T. Makino, S. Arai, H. Tabata, and S. Kawai, *J. Appl. Phys.* **91**, 2290 (2002).
- [15] A. Q. Jiang, J. F. Scott, H. Lu, and Z. Chen, *J. Appl. Phys.* **93**, 1180 (2003).
- [16] S. Rios, A. Ruediger, A. Q. Jiang, J. F. Scott, H. Lu, and Z. Chen, *J. Phys.: Condens. Matter* **15**, L305 (2003).
- [17] K. Antons, J. B. Neaton, K. M. Rabe, and D. Vanderbilt, *Phys. Rev. B* **71**, 024102-1 (2005).
- [18] K. Johnston, X. Huang, J. B. Neaton, and K. M. Rabe, *Phys. Rev. B* **71**, 100103-1 (2005).
- [19] W. Tian, J. C. Jiang, X. Q. Pan, J. H. Haeni, Y. L. Li, L. Q. Chen, D. G. Schlom, J. B. Neaton, K. M. Rabe, and Q. X. Jia, *Appl. Phys. Lett.* **89**, 092905-1 (2006).
- [20] J. Hiltunen, D. Seneviratne, R. Sun, M. Stolfi, H. L. Tuller, J. Lappalainen, and V. Lantto, *Appl. Phys. Lett.* **89**, 242904-1 (2006).
- [21] A. Sarkar and S. B. Krupanidhi, *J. Appl. Phys.* **101**, 104113-1 (2007).
- [22] F. Jona and J. Shirane, *Ferroelectrics crystals*, Pergamon-Press, New York (1962).
- [23] H. Chaib, D. Khatib, and W. Kinase, *Nonlinear Optics* **23**, 97 (2000).
- [24] H. Chaib, L. M. Eng, F. Schlaphof, and T. Otto, *Phys. Rev. B* **71**, 085418-1 (2005).
- [25] H. Chaib, T. Otto, and L. M. Eng, *Phys. Status Solidi B* **23**, 250 (2002); H. Chaib, F. Schlaphof, T. Otto, and L. M. Eng, *J. Phys.: Condens. Matter* **15**, 8927 (2003).
- [26] A. Toumanari, Ph.D. thesis, University of Agadir, Morocco (1999).
- [27] K. Nakamura and W. Kinase, *J. Phys. Soc. Jpn.* **61**, 2114 (1992); K. Nakamura and W. Kinase, *J. Phys. Soc. Jpn.* **61**, 4596 (1992).
- [28] R. S. Cudney, J. Fousek, M. Zgonik, P. Günter, M. H. Garrett, and D. Rytz, *Appl. Phys. Lett.* **63**, 3399 (1993).
- [29] A. R. Johnston and J. M. Weingart, *J. Opt. Soc. Am.* **55**, 828 (1965).
- [30] E. Heifets, R. I. Eglitis, E. A. Kotomin, J. Maier, and G. Borstel, *Phys. Rev. B* **64**, 235417-1 (2001).
- [31] L. Baudry and J. Tournier, *J. Appl. Phys.* **90**, 1442 (2001).
- [32] W. Y. Shih, W. H. Shih, and I. A. Aksay, *Phys. Rev. B* **50**, 15575 (1994).
- [33] W. N. Lawless, *Phys. Rev.* **138**, A1751 (1965).
- [34] K. Ishikawa and T. Uemori, *Phys. Rev. B* **60**, 11841 (1999).
- [35] T. Lu and W. Cao, *Phys. Rev. B* **66**, 024102-1 (2002).
- [36] S. Tinte and M. G. Stachiotti, *Phys. Rev. B* **64**, 235403-1 (2001).